NASA Technical Memorandum 88902

Adhesion, Friction, and Deformation of Ion-Beam-Deposited Boron Nitride Films

Kazuhisa Miyoshi, Donald H. Buckley, Samuel A. Alterovitz,
John J. Pouch, and David C. Liu
Lewis Research Center
Cleveland, Ohio

NASA

ADHESION, FRICTION, AND DEFORMATION OF ION-BEAM-DEPOSITED

BORON NITRIDE FILMS

Kazushisa Miyoshi, Donald H. Buckley, Samuel A. Alterovitz,
John J. Pouch, and David C. Liu
National Aeronautics and Space Administration
Lewis Research Center
Cleveland, Ohio 44135

SYNOPSIS The tribological properties and mechanical strength of boron nitride films were investigated. The BN films were predominantly amorphous and nonstoichiometric and contained small amounts of oxides and carbides. It was found that the yield pressure at full plasticity, the critical load to fracture, and the shear strength of interfacial adhesive bonds (considered as adhesion) depended on the type of metallic substrate on which the BN was deposited. The harder the substrate, the greater the critical load and the adhesion. The yield pressures of the BN film were 12 GPa for the 440C stainless steel substrate, 4.1 GPa for the 304 stainless steel substrate, and 3.3 GPa for the titanium substrate.

1 INTRODUCTION

Considerable research has been conducted on the adhesion, friction, and wear of metals. In recent years the increasing potential for the use of ultrahard, high-temperature materials such as ceramics in tribological systems and in thermodynamically efficient engines (Stirling, adiabatic diesel, and gas turbine) in both terrestrial and space environments has focused attention on these materials.

A promising ceramic material for use as a high-temperature, wear-resistant, solid lubricating film as well as a protective insulator film on semiconductors under a variety of environmental conditions is boron nitride (BN) (1-4).

Boron nitride films can be deposited by a variety of techniques including ion beam deposition (5,6), low-temperature chemical vapor deposition (7,8), plasma deposition (9,10), radiofrequency glow discharge (11), sputtering (12), borazine pyrolysis (13), and others (14). The strength and durability of the films depend largely on the interfacial adhesive bond formed between the film and the substrate.

In this study BN thin films were synthesized by using an ion beam extracted from a borazine $(B_3N_3H_6)$ plasma (6). The films were homogeneously deposited on metallic substrates. The objectives of this study were to investigate the tribological properties and mechanical strength (interfacial adhesive and intrinsic cohesive strength) of hard and brittle BN films deposited on metallic substrates (440C bearing stainless steel, 304 stainless steel, and titanium). The microstructure and chemical composition of the BN film were also examined.

Single-pass scratch experiments were conducted to examine the adhesion, deformation, and fracture behavior of BN films sliding against a diamond pin in air at a relative humidity of 45 per cent and at room temperature.

2 MATERIALS

Thin films containing BN have been synthesized by a commercial firm using an ion beam extracted from a borazine $(B_3N_3H_6)$ plasma (6). The substrates used for scratch experiments and x-ray photoelectron spectroscopy (XPS) analyses were 440C stainless steel, 304 stainless steel, and titanium (99.97 per cent pure) (15). Their surfaces were finished with diamond powder (3-μm particle diam) and with aluminum oxide (1-μm diam) before the BN films were deposited. The BN films on the metallic substrates were approximately 2 μm thick. The substrates used for Auger electron spectroscopy and secondary ion mass spectrometry (AES/SIM) analyses were silicon (3,4).

3 APPARATUS

The ion source used to deposit BN films is described in Ref. 6.

The friction and wear apparatus used in this investigation was capable of scratching the surface of a BN film with a rounded diamond pin (a Rockwell cone diamond with a tip radius of 0.2 mm). The apparatus was commercially purchased (16). A load was applied by placing deadweights on a pan on top of a rod. The other end of the rod contained the diamond pin. A piezoelectric accelerometer mounted just above the diamond pin detected the acoustic emission released as the coating film was disturbed.

The XPS and AES/SIMS systems were also used for chemical composition analyses of the BN films.

4 EXPERIMENTAL PROCEDURE

For the experiments in a laboratory air atmosphere the diamond pin surfaces were scrubbed with levigated alumina (1- and 1/4-μm particle diam) and rinsed with tap water, then with distilled water, and finally with 200-proof ethyl

alcohol before each single-pass sliding experiment. The BN films were also rinsed with 200-proof ethyl alcohol before use. After the surfaces of pin and BN film had been dried with nitrogen gas, the specimens were placed into the friction and wear apparatus. The specimen surfaces were then brought into contact and loaded, and the friction experiment was begun. The time in contact before sliding was 30 sec. Each sliding experiment consisted of a single pass with a total sliding distance of about 10 mm at a sliding velocity of 12 mm/min. The acoustic emission signal was continuously monitored during sliding. The wear tracks formed on the BN films were examined by scanning electron microscopy, optical microscopy, and surface profilometry.

For the surface chemical analyses in vacuum the specimens were placed in vacuum chambers, and the systems were evacuated and baked out to achieve a pressure of 30 nPa (10^{-10} torr) or lower.

The XPS was calibrated regularly. The analyzer calibration was determined by assuming the binding energy for the gold 4f 7/2 peak to be 83.8 eV. The magnesium Kα x-ray was used with an x-ray source power of 400 W (10 kV; 40 mA). The spectra were obtained with a pass energy of 25, 50, or 100 eV. The XPS was used in conjunction with argon ion sputtering to clean the specimens. Ion-sputter etching was performed with a beam energy of 3 keV at 20-mA beam current with an argon pressure of 0.7 mPa. The ion beam was continuously rastered over the specimen surface. After sputter etching the system was reevacuated to a pressure of 30 nPa or lower. The relative atomic concentrations of the various constituents on the BN film surfaces analyzed by XPS were determined by using peak area (atomic) sensitivity factors and the relative peak areas of photoelectrons (17).

Compositional depth profiles of a BN film deposited on a silicon substrate were obtained by using the AES/SIMS system. Ion sputter etching was performed with 3-keV argon ions. Absolute etch rates were determined by comparison with ellipsometrically determined film thicknesses. Absolute values of the atomic concentrations were obtained by correcting the peak-to-peak signal amplitude by the corresponding elemental sensitivity factor (18). The microstructure of the BN film was examined by transmission electron microscopy and diffraction in a microscope operating at 100 kV. BN films were removed from the substrates by mechanical methods including ion etching.

5 RESULTS AND DISCUSSION

5.1 Microstructure

A typical transmission electron photomicrograph (Fig. 1(a)) indicates that the BN film lacked the macroscopic structural features common in both the monolithic cubic and hexagonal forms of BN. In the absence of macroscopic crystallinity neither grains, grain boundaries, grain orientations, nor additional phases were found to exist. The electron diffraction pattern of the film (Fig. 1(b)) indicates a diffused ring structure containing three rings that were identified as hexagonal (BN)4H. This evidence suggests the presence, in addition to a structureless amorphous phase, of a crystalline phase with a size

range of 8 to 30 nm. That is, the films were not completely amorphous; properties characteristic of hexagonal BN were detected. This finding agrees with electron microscopical and optical band gap observations (3,4).

5.2 Chemical composition

XPS survey spectra (scans of 1100 eV) of the BN film surfaces on the substrates obtained before sputter cleaning typically revealed a carbon peak as well as an adsorbed oxygen peak, as shown by curves (a) in Fig. 2. A layer of adsorbate on the surface consisted of water vapor and hydrocarbons from the atmospheric environment that may have condensed and become physically adsorbed to the BN film. After BN film surfaces had been argon ion sputter cleaned for 45 min, small carbon and oxygen contamination peaks as well as boron and nitrogen remained (curves (b) in Fig. 2).

The B_{1s} photoelectron emission lines of the BN (Fig. 2) peaked primarily at 190 eV, which is associated with BN. They also included a small amount of B_4C. The N_{1s} photoelectron lines for the BN peaked primarily at 397.9 eV, which is again associated with BN. The C_{1s} photoelectron lines taken from the as-received surface at 284.6 eV indicate the presence of adventitious adsorbed carbon contamination with a small amount of carbides. After sputter cleaning the adsorbed carbon contamination peak disappeared from the spectrum, and the relatively small carbide peak could be seen. The O_{1s} photoelectron lines of the as-received BN surface peaked at 531.6 eV because of adsorbed oxygen contamination and oxides. After sputter cleaning the adsorbed oxygen contamination peak disappeared from the spectrum, but the small oxide peak remained.

The peak intensity for both boron and nitrogen associated with BN increased with argon ion sputter cleaning; that for carbon and oxygen decreased markedly. The BN film deposited on the 440C substrate was nonstoichiometric, with a B/N ratio of 1.6 (~2).

Elemental depth profiles for the ion-beam-deposited BN film on silicon were obtained as a function of the sputtering time from AES analyses (Fig. 3). The height of the boron and nitrogen peaks rapidly increased with an increase in the sputtering time. The oxygen and carbon peaks, however, decreased in the first 1 to 2 min and remained constant thereafter. The BN film deposited on silicon had a B/N ratio of about 2. Thus XPS and AES analyses clearly revealed that BN was nonstoichiometric and small amounts of oxides and carbides were present on the surface and in the bulk of the BN film. Contaminants such as carbides (e.g., B_4C) and oxides may be introduced and absorbed in the BN film during ion beam synthesis.

The BN films deposited on silicon substrates were probed by SIMS. The spectra indicated the presence of the following secondary ions: B^+, B_2^+, C^+, O^+, Si^+, Si_2^+, and SiO^+. The peak observed at 14 amu could result from N^+, CH_2^+, and Si_2^+. Additional peaks at 24 and 25 amu were related to BN^+ and thus supported the XPS data. The SiO^+ signal was associated with the oxide, which was present at the BN-Si interface.

5.3 Deformation and fracture

A series of scratch experiments were conducted with BN films on 440C stainless steel, 304 stainless steel, and titanium flat substrates sliding against diamond pins in laboratory air. Comparative experiments were also conducted with 440C stainless steel and titanium sliding against diamond pins in laboratory air.

When a BN film surface is brought into sliding contact with a diamond under relatively small load (<2 N), elastic deformation can occur locally in both the BN film and the diamond. Sliding occurs at the interface. However, in these experiments no permanent groove formation due to plastic flow and no cracking of the BN film with sliding were observed. An increase (of a few newtons) in load, however, resulted in plastic deformation of the BN film. The diamond indented and slid on the BN film without itself suffering permanent deformation, but it caused permanent grooves in the BN film and substrate during sliding. The BN film deformed plastically much like metallic films.

When a much higher load was applied on a BN film, however, the sliding action produced locally gross surface and subsurface fracturing in the film. Scanning electron photomicrographs of a wear track on a BN film deposited on a 304 stainless steel substrate (Fig. 4) reveal that both plastic deformation and fracture occurred in the BN film. The fracturing resulted from brittle cracks being generated, propagated, and then intersected in the BN film and at the interface between the BN film and the substrate. The backscatter photomicrograph (Fig. 4(b)) reveals two different materials: (1) the BN film stayed on the substrate (dark areas in the photomicrograph) and (2) the BN film fragments came off revealing the 304 stainless steel substrate (light areas).

Scanning electron photomicrographs of a wear track on a BN film deposited on a 440C stainless steel substrate (Fig. 5) reveal that the BN film deformed plastically during sliding at a load of 1.1 N. Permanent grooves were formed where the diamond began to slide (Fig. 5(b)). However, the sliding action also produced sudden gross flaking of the BN film. A large light area in the last half of the wear track (Fig. 5(a)) is a fracture pit where the BN film was completely removed along the sliding direction of the diamond. This is confirmed by the backscatter photomicrograph (Fig. 5(c)), which shows the light area to be the 440C stainless steel substrate. The fracturing and removal of the BN film from the 440C substrate were caused by fracture of cohesive bonds in the BN film and interfacial adhesive bonds between the film and the substrate in and near the contact region with the diamond. The BN film was fractured and removed from the titanium substrate in a similar manner.

Acoustic emission is released and detected when adhesive bonds between the BN film and the substrate or intrinsic cohesive bonds in the BN film are broken and new surface is created. The pattern and intensity of the acoustic emission depend on the nature of the disturbance: cracking, flaking of chevron-shaped fragments, or flaking of irregular-shaped fragments, etc. (16).

Typical acoustic emission traces for a BN film on a metallic substrate measured at loads of 6, 8, and 10 N are presented in Fig. 6. No acoustic emission was detected at loads of 6 N or less. Traces for loads higher than 8 N, which are the critical loads to fracture for a BN film deposited on a titanium substrate, clearly indicated evidence of acoustic emission signal output. The acoustic emission was released as the BN film was disturbed. Such acoustic emission is due to the sudden release of elastic energy when cracks propagate to the coating-substrate interface (16). In general the acoustic emission signal level increased with an increase in load, as demonstrated in Fig. 6. Thus the critical load to fracture of a BN film on a metal substrate can be detected by an acoustic emission technique. Although the failure modes for BN films differed with the metallic substrate, the critical loads obtained acoustically agreed well with those detected by optical and SEM microscopy of the scratches.

5.4 Yield pressure and Meyer's law

The foregoing results revealed that the sliding action of the diamond results in a permanent groove in the BN film at certain loads. Scratch measurements were therefore conducted with a BN film deposited on the substrates, starting from the smallest loads at which the scratches were visible by optical microscopy and detectable by surface profilometry.

The width D and height H of a groove with some amount of deformed BN piled up along its sides are defined in Fig. 7. The widths of the grooves reported herein were obtained by averaging the widths from 10 or more measurements of surface profile traces or of optical microscopy. Mean contact pressure (yield pressure) P during sliding may then be defined by $P = W/A_s$, where W is the applied load and A_s is the projected contact area and is given by $A_s = D^2/8$ (only the front half of the pin is in contact with the flat) (19).

The yield pressure over the contact area gradually rose until the deformation passed to a "fully plastic state" (Table 1). The mean contact pressure at a fully plastic state P_m is higher than (by about 25 per cent) but proportional to the measured Vickers hardness (16).

The relation between the load and the width of the resulting scratch may be expressed by a number derived from empirical relations (20). When the width of the resulting scratch D for BN films is plotted against the load W on logarithmic coordinates, this is expressed by $W = kD^n$ (i.e., Meyer's law, as typically presented in Fig. 8).

Figure 8 presents data for scratch widths obtained for BN films on 440C stainless steel, 304 stainless steel, and titanium substrates. Comparative data for uncoated 440C stainless steel, 304 stainless steel, and titanium themselves are also presented. The portion LM for BN films or L'M' for uncoated metallic materials is gradually curved but is considered to be composed of approximately straight portions of transitional slopes. For example, the transitional slopes are 2.6 and 2.2 for BN film on 440C stainless steel. The portion MN for BN films or M'N' for uncoated metals is a straight line of slope 2. It is evident that MN or M'N' is the range over which Meyer's law is valid for BN

3

films on metallic substrates and for uncoated metallic materials. Here the Meyer index n is constant and has the value 2. Thus the BN films on metallic substrates behave plastically much like metals when they are brought into contact with hard solids such as diamond.

As discussed earlier, however, when the load exceeds a certain critical value, the sliding action produces locally gross surface and subsurface fracturing in the BN film on the metallic substrates. The critical load to fracture depends strongly on the substrate. The critical loads to fracture the BN film on 440C stainless steel, 304 stainless steel, and titanium were 1.1, 0.7, and 0.8 N, respectively (Fig. 8 and Table 1).

It is interesting to note that the portion FF, representing the condition of fracture where the load exceeded the critical load, is roughly expressed by $W = kD^n$ in Fig. 8. The fractured scratch for the BN film on the substrate was almost as wide as that for the uncoated metallic material used for the substrate. This evidence confirms that cracks are generated from the contact area rather than from the free surface of the film. It suggests that the substrate is responsible not only for controlling the critical load to fracture the BN film but for the extent of fracture as well.

5.5 Adhesion and shear strength

Either interfacial adhesive bonds between the coating and the substrate or cohesive bonds in the BN coating were broken when critically loaded. For example, with 440C stainless steel and titanium some of the interfacial adhesive bonds between the BN film and the substrate were generally weaker than the cohesive bonds in the BN film. The failed surface revealed the complete removal of the BN film from the 440C stainless steel surface or the titanium surface (Fig. 5).

On the other hand, with the 304 stainless steel substrate the interfacial adhesive bonds between the BN film and the substrate were generally stronger than the cohesive bonds in the BN film. The BN film first cracked when it was critically loaded. The failure of the BN film induced fracture of interfacial adhesive bonds between it and the substrate, and the BN film fragments were partially removed from the substrate.

Although the failure modes observed with the BN films on 440C stainless steel, 304 stainless steel, and titanium were different, Fig. 8 suggests that the shear strength, considered as the adhesion strength of the interfacial bonds between the BN film and the substrate, was related to the mechanical strength of the substrate.

Benjamin and Weaver (21) had derived the following expressions for scratch adhesion in terms of shearing stress S produced at the coating-substrate interface by the plastic deformation, the hardness of the substrate (yield pressure at fully plastic state P_m), the critical load applied on the pin W_c, and the tip radius of the pin R:

$$S = K\left(\frac{W_c P_m}{\pi R^2}\right)^{1/2} \qquad (1)$$

$$S \simeq \frac{2W_c}{\pi DR} \qquad (2)$$

These relations allow for the calculation of the shear strength (i.e., the adhesion strength of the interfacial bonds (21, 19)). The results are presented in Table 1. The values of the critical loads were obtained and confirmed not only by optical and SEM microscopy of the scratches, but also by the acoustic emission technique. The hardnesses of the metallic substrates were obtained from the data on uncoated metallic materials. Table 1 reveals generally the strong correlation between the shear strength (i.e., adhesion) and the hardness of the substrate. The harder the metallic substrate, the greater the shear strength.

6 CONCLUSIONS

As a result of single-pass scratch experiments conducted with boron nitride (BN) films on 440C stainless steel, 304 stainless steel, and titanium substrates in sliding contact with a diamond pin, the following conclusions were drawn:

1. Ion-beam-deposited BN films are not completely amorphous but contain (to a small extent) hexagonal BN.

2. The surfaces of sputter-cleaned BN films are nonstoichiometric, with a B/N ratio of approximately 2, and contain small amounts of oxides and carbides in addition to BN.

3. BN films, like metal films, deform elastically and plastically in the interfacial region between two solids in contact under load. Unlike metal films, however, when critically loaded, BN films can fracture.

4. The yield pressures at a fully plastic state are 12 GPa (1200 kg/mm^2) for BN film on 440C stainless steel, 4.1 GPa (420 kg/mm^2) for BN film on 304 stainless steel, and 3.3 GPa (340 kg/mm^2) for BN film on titanium.

5. The relation between the load W and the width of the plastically deformed groove D for BN films is expressed by $W = kD^n$ (i.e., the classical Meyer's law).

6. The critical load required to fracture a BN film on a metallic substrate obtained acoustically agrees well with those detected by optical and SEM microscopy of the scratches. The critical load increases with increasing hardness of the substrate.

7. There appears to be strong correlation between the shear strength of interfacial adhesive bonds (considered as adhesion) and the hardness of the substrate. The harder the metallic substrate, the greater the shear strength.

REFERENCES

1. MIYOSHI, K. and BUCKLEY, D.H., Microstructure and Surface Chemistry of Amorphous Alloys Important to Their Friction and Wear Behavior. Wear, 1986, 110, 295-313.

4

2. BUCKLEY, D.H., Friction and Transfer Behavior of Pyrolytic Boron Nitride in Contact with Various Metals. ASLE Trans, 1978, 21, 118-124.

3. ALTEROVITZ, S.A., WARNER, J.D., LIU, D.C. and POUCH J.J., Ellipsometric and Optical Study of Some Uncommon Insulator Films on III-V Semiconductors. Proceedings of the Symposium on Electric Films on Compound Semiconductors, V.J. Kapoor, D.J. Connolly and Y.H. Wong, eds., Electrochemical Society, Pennington, 1986, 59-77.

4. POUCH, J.J., ALTEROVITZ, S.A. and WARNER, J.D., Auger Electron Spectroscopy, Secondary Ion Mass Spectrometry and Optical Characterization of a-C:H and BN Films. NASA TM-87258, 1986.

5. WEISSMANTEL, C., Ion-Beam Deposition of Special Film Structures. J. Vac. Sci. Technol., 1981, 18, 179-185.

6. SHANFIELD, S. and WOLFSON, R., Ion-Ceam Synthesis of Cubic Boron Nitride. J. Vac. Sci. Technol. A, 1983, 1, 323-325.

7. MOTOJIMA, S., TAMURA, Y. and SUGIYAMA, K., Low Temperature Deposition of Hexagonal BN Films by Chemical Vapor Deposition. Thin Solid Films, 1982, 88, 269-274.

8. MURAKA, S.P., CHENG, C.C., WANG, D.N.K. and SMITH, T.E., Effect of Growth Parameters on the CVD of Boron Nitride and Phosphorous-Doped Boron Nitride. J. Electrochem. Soc., 1979, 126, 1951-1957.

9. HYDER, S.B. and YEP, T.O., Structure and Properties of Boron Nitride Films Grown by High Temperature Reactive Plasma Deposition. J. Electrochem. Soc., 1976, 123, 1721-1724.

10. LIU, D.C., VALCO, G.J., SKEBE, G.G. and KAPOOR, V.J., Plasma-Deposited Nitride Films on Gallium Arsenide and Indium Phosphide. Proceedings of the Symposium on Silicon Nitride Thin Insulating Films, V.J. Kapoor and H.J. Stein, eds., Electrochemical Society, Pennington, 1983, 141-149.

11. MIYAMOTO, H., HIROSE, M. and OSAKA, Y., Structural and Electronic Characterization of Discharge-Produced Boron Nitride. Jpn. J. Appl. Phys. Part 2, 1983, 22, L216-L218.

12. WIGGINS, M.D. and AITA, C.R., Radio Frequency Sputter Deposited Boron Nitride Films. J. Vac. Sci. Technol. A, 1984, 2, 322-325.

13. ADAMS, A.C., Characterization of Films Formed by Pyrolysis of Borazine. J. Electrochem. Soc., 1981, 128, 1378-1379.

14. NAKAMURA, K. Preparation and Properties of Amorphous Boron Nitride Films by Molecular Flow Chemical Vapor Deposition. J. Electrochem. Soc., 1985, 132, 1757-1762.

15. MIYOSHI, K., BUCKLEY, D.H. and SPALVINS, T., Tribological Properties of Boron Nitride Synthesized by Ion Beam Deposition. J. Vac. Sci. Technol. A, 1985, 3, 2340-2344.

16. HINTERMANN, H.E., Surface Treatments. Science of Hard Materials, R.K. Viswanadham, D.J. Rowcliffe and J. Gorland, eds., Plenum, New York, 1983, 357-394.

17. WAGNER, C.D. and MUILENBERG, G., eds., Handbook of X-Ray Photoelectron Spectroscopy, Perkin-Elmer Corp., Eden Prairie, 1979.

18. DAVIS, L.E., MACDONALD, N.C., PALMBERG, P.W., RIACH, G.E. and WEBER, R.E., Handbook of Auger Electron Spectroscopy, 2nd edition. Perkin-Elmer Corp., Eden Prairie, 1976.

19. AHN, J., MITTAL, K.L. and MACQUEEN, R.H., Hardness and Adhesion of Filmed Structures as Determined by the Scratch Technique. Adhesion Measurements of Thin Films, Thick Films, and Bulk Coatings, K.L. Mittal, ed., ASTM Special Technical Publication 640 (1978) 134-157.

20. TABOR, D., The Hardness of Metals, Clarendon Press, Oxford, 1951.

21. BENJAMIN, P. and WEAVER, C., Measurement of Adhesion of Thin Films. Proc. R. Soc. London A, 1960, 254, 163-176.

Table 1 Critical normal load to fracture BN film in sliding contact and shear strength of interfacial adhesive bonds

Substrate	Hardness of substrate		Yield pressure at a fully plastic state, P_m		Critical normal load, W_c, N	Interfacial adhesive strength, S			
						From eq. (1)		From eq. (2)	
	GPa	kg/mm²	GPa	kg/mm²		GPa	kg/mm²	GPa	kg/mm²
440C stainless steel	7.1	720	12	1200	1.1	0.77	79	0.68	69
304 stainless steel	2.5	255	4.1	420	.7	.37	38	.29	30
Titanium	2.6	270	3.3	340	.8	.40	41	.30	31
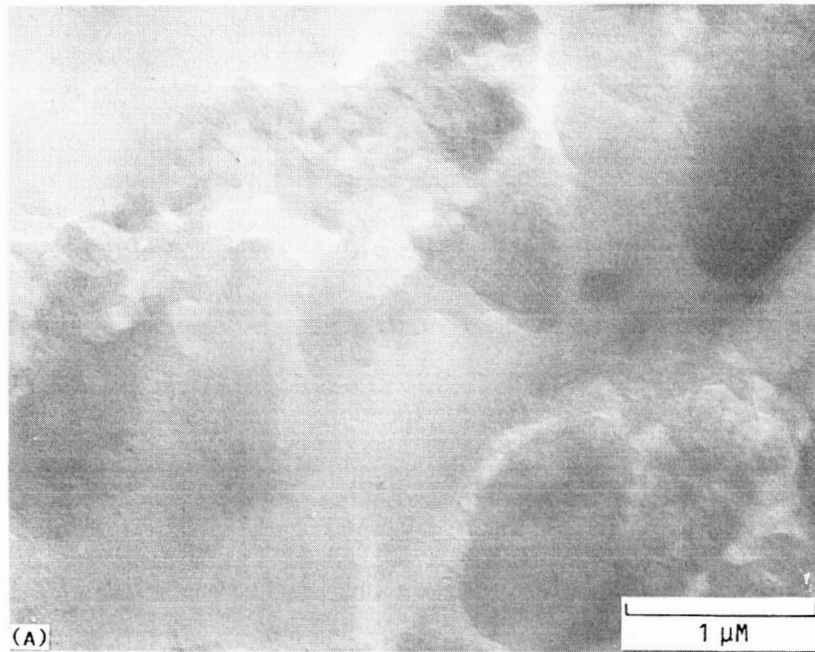
(A) TRANSMISSION ELECTRON MICROGRAPH.
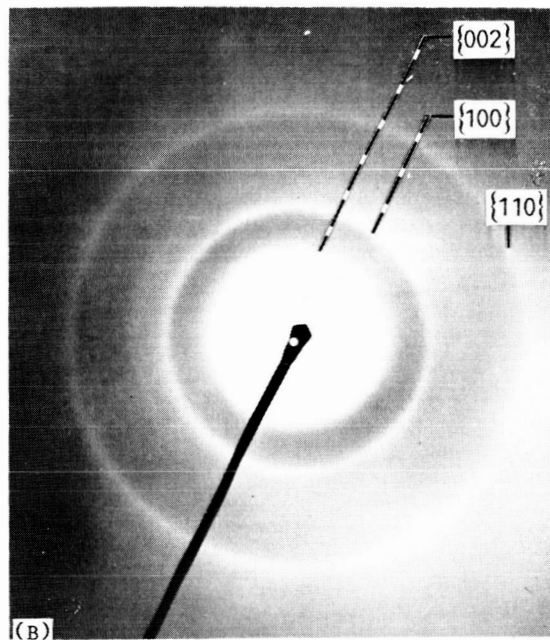
(B) ELECTRON DIFFRACTION PATTERN.

FIGURE 1. – TYPICAL MICROSTRUCTURE AND ELECTRON DIFFRACTION
PATTERN OF BN COATING FILM.

(A) BEFORE ION SPUTTERING.

(B) AFTER ION SPUTTERING.
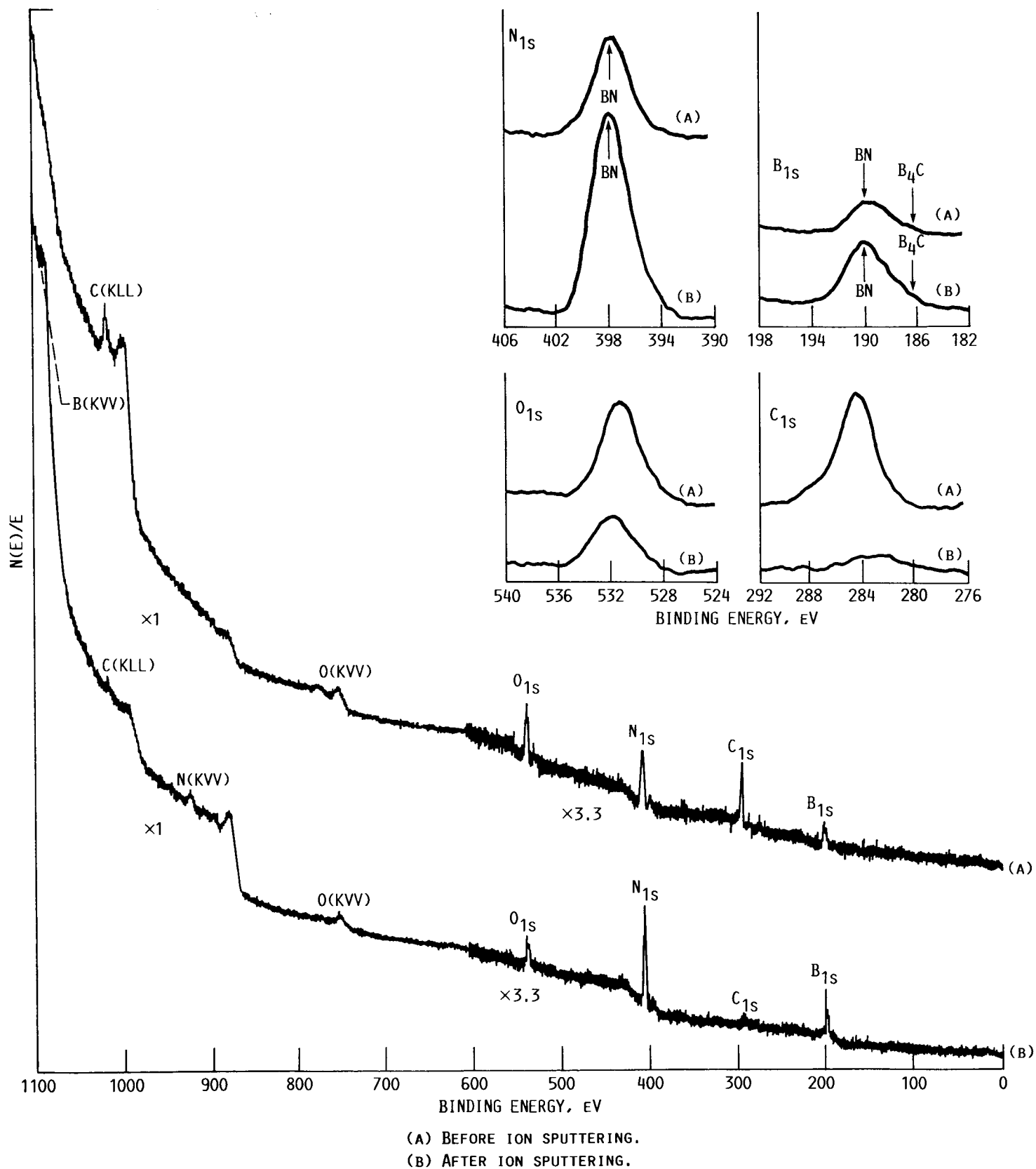
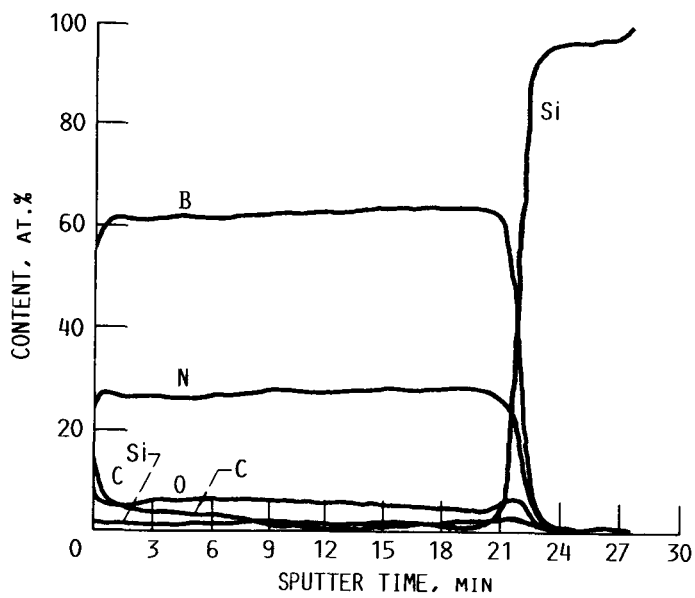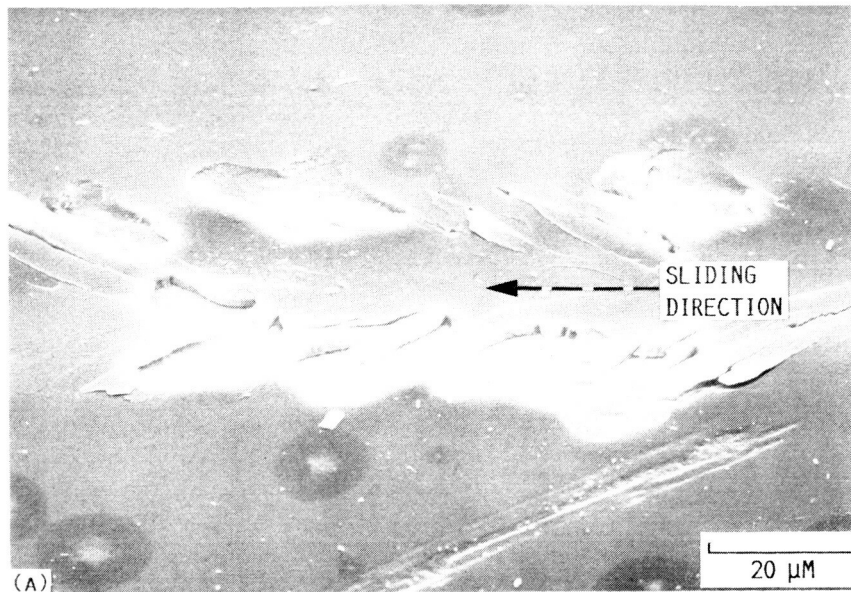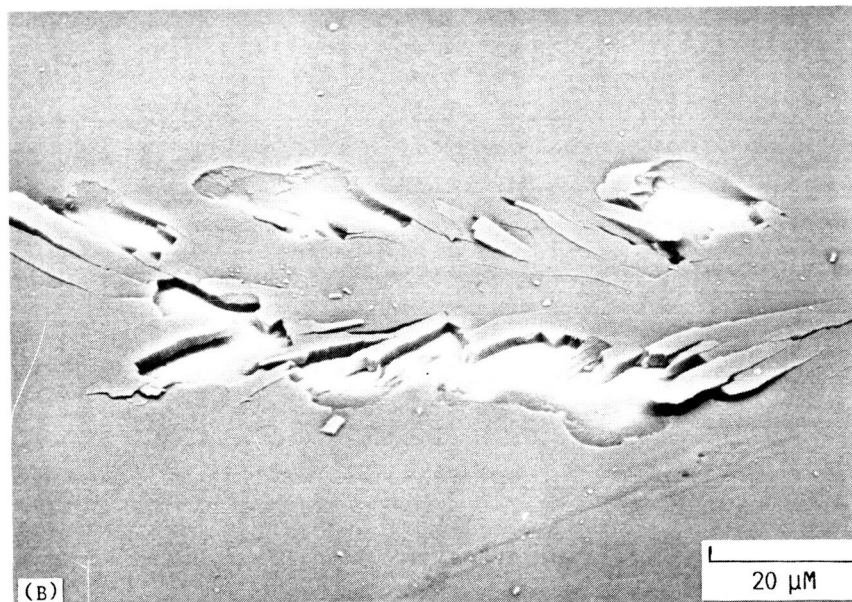FIGURE 2. - XPS SPECTRA OF ION-BEAM-DEPOSITED BN FILM (SPUTTERING TIME, 45 MIN; SUBSTRATE, 440C STAINLESS STEEL).

FIGURE 3. - AES ATOMIC PERCENT AS A FUNCTION OF
SPUTTER TIME FOR ION-BEAM-DEPOSITED BN FILM
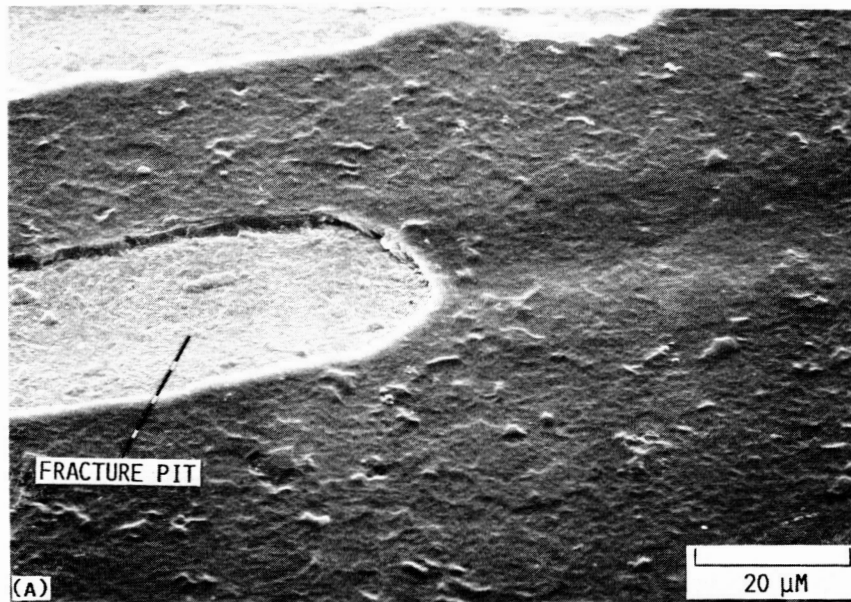ON SI (DEPOSITION TEMPERATURE, 200 ^OC; ION
BEAM ENERGY, 150 EV).
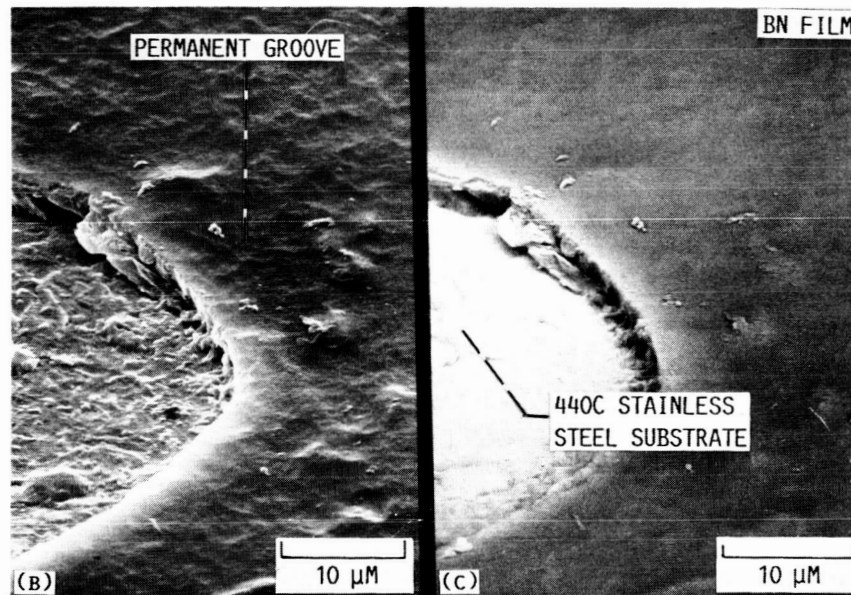
(A) SECONDARY ELECTRON IMAGE SEM.

(B) BACKSCATTER ELECTRON IMAGE SEM.

FIGURE 4. – SCANNING ELECTRON PHOTOMICREOGRAPHS OF WEAR ON BN FILM SURFACE
GENERATED BY 0.2-MM-RADIUS DIAMOND PIN. SUBSTRATE, 304 STAINLESS STEEL;
LOAD, 0.7 N; SLIDING VELOCITY, 12 MM/MIN; LABORATORY AIR.

(A) SECONDARY ELECTRON IMAGE SEM (LOW MAGNIFICATION).

(B) SECONDARY ELECTRON IMAGE SEM (HIGH MAGNIFICATION).
(C) BACKSCATTER ELECTRON IMAGE SEM.

FIGURE 5. – SCANNING ELECTRON PHOTOMICROGRAPHS OF WEAR TRACK ON BN FILM
SURFACE GENERATED BY 0.2-MM-RADIUS DIAMOND PIN. SRBSTRATE, 440C STAINLESS
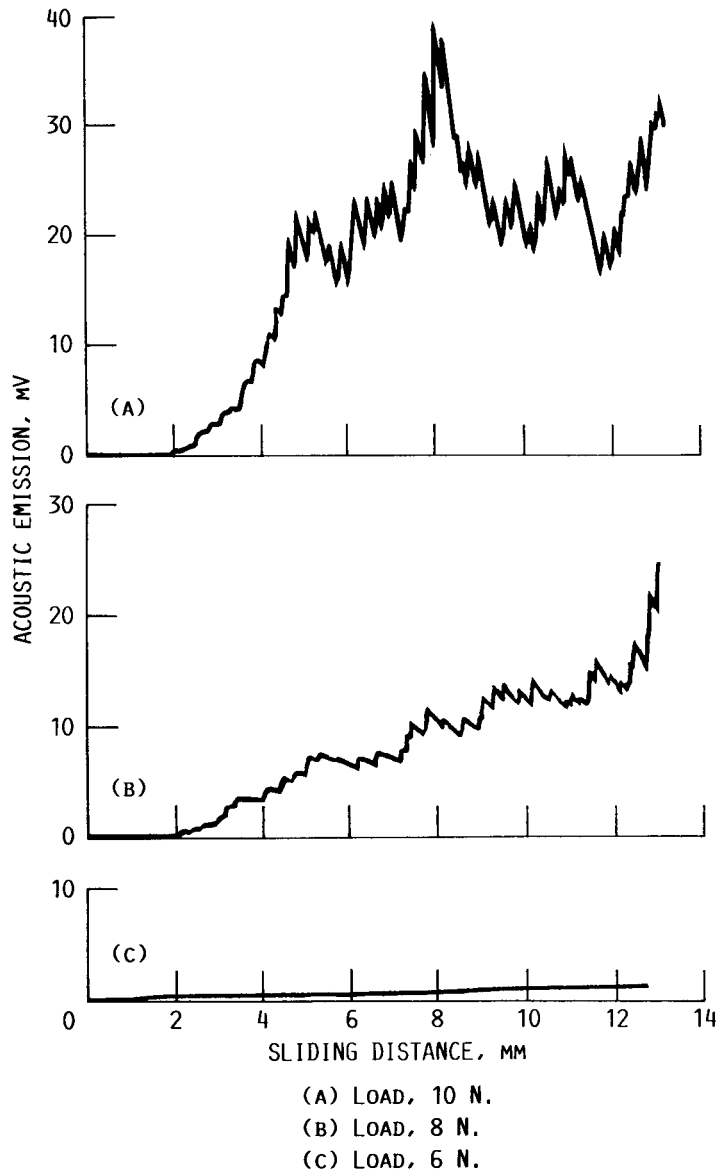STEEL; LOAD, 1.1 N; SLIDING VELOCITY, 12 MM/MIN; LABORATORY AIR.

(A) Load, 10 N.
(B) Load, 8 N.
(C) Load, 6 N.

Figure 6. - Typical acoustic emission traces for a BN film on a metal (substrate, titanium; sliding velocity, 12 mm/min; laboratory air).
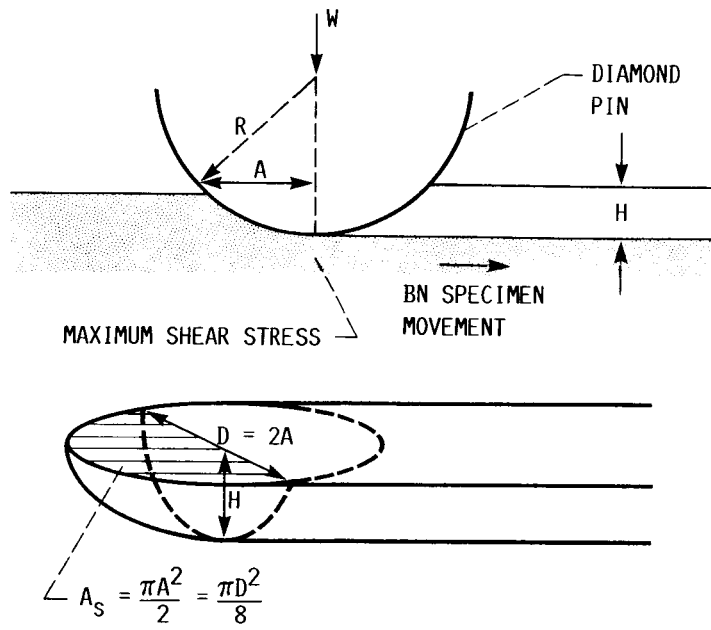
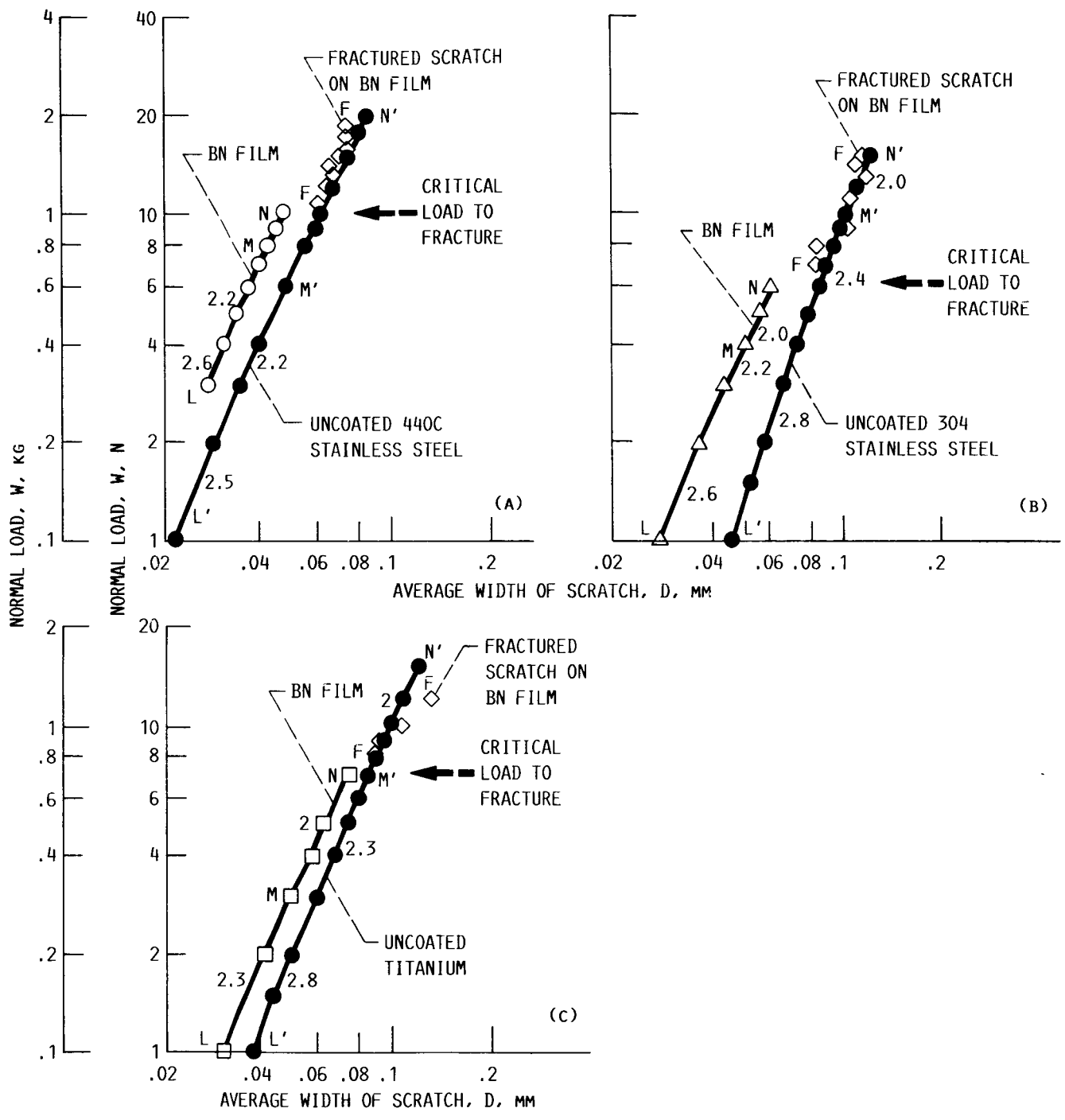$$A_s = \frac{\pi A^2}{2} = \frac{\pi D^2}{8}$$

FIGURE 7. - DEFINITION OF MEAN CONTACT PRESSURE
($P = W/A_s$), OR SCRATCH HARDNESS.

(A) BN FILM ON 440C STAINLESS STEEL.
(B) BN FILM ON 304 STAINLESS STEEL AND UNCOATED 304 STAINLESS STEEL.
(C) BN FILM ON TITANIUM AND UNCOATED TITANIUM.

FIGURE 8. - SCRATCH WIDTH AS A FUNCTION OF LOAD (SLIDING VELOCITY, 12 MM/MIN; LABORATORY AIR).

1. Report No. NASA TM-88902	2. Government Accession No.	3. Recipient's Catalog No.
4. Title and Subtitle Adhesion, Friction, and Deformation of Ion-Beam-Deposited Boron Nitride Films		5. Report Date 6. Performing Organization Code 506-43-11
7. Author(s) Kazushisa Miyoshi, Donald H. Buckley, Samuel A. Alterovitz, John J. Pouch, and David C. Liu		8. Performing Organization Report No. E-3326
		10. Work Unit No.
9. Performing Organization Name and Address National Aeronautics and Space Administration Lewis Research Center Cleveland, Ohio 44135		11. Contract or Grant No.
		13. Type of Report and Period Covered Technical Memorandum
12. Sponsoring Agency Name and Address National Aeronautics and Space Administration Washington, D.C. 20546		14. Sponsoring Agency Code

15. Supplementary Notes

Prepared for the International Conference on Tribology, sponsored by the Institution of Mechanical Engineers, London, England, July 1-3, 1987.

16. Abstract

The tribological properties and mechanical strength of boron nitride films were investigated. The BN films were predominantly amorphous and nonstoichiometric and contained small amounts of oxides and carbides. It was found that the yield pressure at full plasticity, the critical load to fracture, and the shear strength of interfacial adhesive bonds (considered as adhesion) depended on the type of metallic substrate on which the BN was deposited. The harder the substrate, the greater the critical load and the adhesion. The yield pressures of the BN film were 12 GPa for the 440C stainless steel substrate, 4.1 GPa for the 304 stainless steel substrate, and 3.3 GPa for the titanium substrate.

17. Key Words (Suggested by Author(s)) Adhesion; Deformation; BN films	18. Distribution Statement Unclassified – unlimited STAR Category 27

19. Security Classif. (of this report) Unclassified	20. Security Classif. (of this page) Unclassified	21. No. of pages	22. Price*

*For sale by the National Technical Information Service, Springfield, Virginia 22161